



OPEN Phenylacetylcarbinol biotransformation by disrupted yeast cells using ultrasonic treatment in conjunction with a dipropylene glycol mediated biphasic emulsion system

Rojarej Nunta^{1,4}, Kritsadaporn Porninta^{1,2}, Sumeth Sommanee^{1,2}, Chatchadaporn Mahakuntha^{1,2}, Charin Techapun^{1,2}, Juan Feng^{1,2}, Su Lwin Htike^{1,2}, Julaluk Khemacheewakul^{1,2}, Yuthana Phimolsiripol^{1,2}, Kittisak Jantanasakulwong^{1,2}, Pornchai Rachtanapun^{1,2}, Usa Bostong⁴, Anbarasu Kumar^{1,2,3}✉ & Noppol Leksawasdi^{1,2}✉

Biotransformation of a pharmaceutical precursor, phenylacetylcarbinol (PAC), could be achieved by frozen-thawed *Candida tropicalis* whole cells (FT-WHC). The treatment of FT-WHC, which contained intracellular pyruvate decarboxylase (PDC) enzyme, using high-power ultrasonication with varying amplitudes were compared with glass bead attrition (GBA) as well as control for the release of PDC. Ultrasonication at 20% amplitude (Ult20) proved to be the most effective, resulting in the highest volumetric and specific PDC activities of 0.210 ± 0.004 U/mL and 0.335 ± 0.033 U/mg protein, respectively. Disrupted FT-WHC using Ult20 exhibited a statistically significant ($p \leq 0.05$) higher initial PAC production rate (3.26 ± 0.04 mM). The comparison of three organic phases, namely, vegetable oil (Vg-Oil), Vg-Oil + dipropylene glycol (DPG), and octanol in the two-phase emulsion system for PAC biotransformation revealed the highest statistically significant ($p \leq 0.05$) overall PAC concentration of 28.9 ± 0.1 mM in Vg-Oil + DPG system. The novel addition of DPG helped facilitating the partitioning of PAC into aqueous phase, stabilizing specific PDC activity, and specific PAC productivity in combination with ultrasonication treatment.

Keywords High value-added chemical, Biotransformation, Pyruvate decarboxylase, Sustainable agriculture, Resource efficiency, Recycling

Abbreviations

[]	Concentration
aq	Aqueous phase
Bz	Benzaldehyde
Bzc	Benzoic acid
DPG	Dipropylene glycol
FLJ-C	Fresh C-grade longan juice
FT-WHC	Frozen-thawed yeast whole cells
GB	Glass beads
GBA	Glass bead attrition

¹Center of Excellence, Agro-Bio-Circular-Green Industry (Agro-BCG) & Bioprocess Research Cluster (BRC), School of Agro-Industry, Faculty of Agro-Industry, Chiang Mai University, Chiang Mai 50100, Thailand. ²Faculty of Agro-Industry, Chiang Mai University, Chiang Mai 50100, Thailand. ³Department of Biotechnology, Periyar Maniammai Institute of Science & Technology (Deemed to Be University), Thanjavur 613403, India. ⁴Division of Food Innovation and Business, Faculty of Agricultural Technology, Lampang Rajabhat University, Lampang 52100, Thailand. ✉email: anbarasuk@pmu.edu; noppol@hotmail.com

HPLC	High performance liquid chromatography
MOPS	3-(N-Morpholino) propanesulfonic acid
org	Organic phase
PAC	Phenylacetylcarbinol
PDC	Pyruvate decarboxylase
Pyr	Pyruvate
$Q_{PAC,ini}$	Initial PAC productivity at 5 min (mM/min)
$Q_{PAC,fin}$	Final PAC productivity at 360 min (mM/min)
$Q_{PAC,max}$	Maximum PAC productivity during the biotransformation time course (mM/min)
Spc.	Specific
$S_{p,PAC}$	Specific PAC production ($\mu\text{mol/Uini}$)
TISTR	Thailand Institute of Scientific and Technological Research
Ult	Ultrasonication
U_{ini}	Initial volumetric PDC activity
Vol.	Volumetric
YPD	Yeast extract-peptone-dextrose

Phenylacetylcarbinol (PAC) is a valuable precursor (USD 120/kg¹) for the synthesis of ephedrine and pseudoephedrine, which are used as decongestants and bronchodilators². PAC is produced through a biotransformation process involving yeast pyruvate decarboxylase (PDC) enzyme. In this process, pyruvate, an intermediate in glycolysis, undergoes decarboxylation catalyzed by PDC, forming an acetaldehyde intermediate. Subsequently, benzaldehyde reacts with this intermediate to yield PAC^{3,4}. The involvement of PDC is crucial as it initiates the decarboxylation of pyruvate, allowing the formation of the reactive intermediate essential for PAC synthesis.

Past research has leveraged the advantages of whole cell yeasts as biocatalysts, particularly as a source of PDC in PAC production^{5–9}. Biocatalytic systems based on whole cells have gained prominence, offering advantages over isolated enzymatic systems^{10,11}. Notably, the elimination of expensive and time-consuming downstream processes, including enzyme purification, represents a significant benefit. Yeasts, as a subset of whole-cell biocatalysts, have emerged as traditional and versatile options¹². Yeast cells, capable of expressing diverse enzymatic activities, are easily produced and managed, demonstrating stability and typically being non-pathogenic. The study conducted by Khemacheewakul et al.⁹ focused on the production of PAC using whole cells of *Candida tropicalis* – the highest PAC production strain¹³. The authors evaluated buffer concentrations for efficient PAC production and buffer concentration's impact on the deactivation kinetics of whole cells PDC activity. In another study, Nunta et al.⁵ employed the whole cells of *C. tropicalis* TISTR 5306 and *Saccharomyces cerevisiae* TISTR 5606 to produce PAC. The study revealed a statistically significant ($p \leq 0.05$) difference in PAC levels, with *C. tropicalis* whole cells exhibiting higher levels compared to *S. cerevisiae*. Latest study from Htike et al.¹⁴ indicated that three strains of *Candida* spp., namely *C. tropicalis*, *C. magnoliae*, and *C. guilliermondii*, showed a similar PAC concentration in the range of 14.4 – 14.7 mM under a single-phase system of phosphate buffer. In a recent investigation by Nunta et al.⁸, a comparison was made between the biomass of whole cells from *C. tropicalis* and a partially purified PDC preparation for the biotransformation of PAC. The whole cells of *C. tropicalis*, containing PDC at a concentration of 1.29 U/mL, yielded a total PAC concentration that was 68.4% greater compared to the outcome obtained with the partially purified enzyme preparation. Having established the efficacy of yeast whole cells, particularly those derived from strains like *C. tropicalis* or *S. cerevisiae*, in PAC biotransformation, the exploration of disrupted yeast whole cells can further enhance the potential of this approach. Disruption of yeast cells introduces additional advantages, such as enhanced enzyme accessibility, increased surface area, improved mass transfer, and simplified downstream processing. These advantages make disrupted yeast cells a compelling choice for researchers seeking to optimize and broaden the scope of PAC biotransformation processes^{6,7}.

Nevertheless, it is imperative to disrupt the structures of microbial cells because microorganisms consist of a robust external cell wall, a cytoplasmic membrane, and an intricate cytoplasm housing vital biomolecules and water¹⁵. Therefore, methods for disrupting cells can be employed to enhance the membrane permeability or facilitate the leakage of cellular contents. Various disruption techniques can be used including mechanical methods such as homogenization, pressure-based cell rupture, sonication, and freezing and thawing¹⁶; enzymatic methods involving specific enzymes to break down cell components; and chemical methods using detergents, silver nanoparticles, or solvents to disrupt cells integrity^{7,15}. These cell disruption methods are indispensable in biotransformation studies and biotechnology, enabling the extraction of nucleic acids, proteins, carbohydrates, lipids, enzymes, and other valuable substances for further research and applications.

Comparing to whole-cell immobilization and immobilized enzymes which might offer enhanced stability and reusability of biocatalysts during biotransformation, some drawbacks do exist such as mass transfer limitation, decrease in substrates accessibility, and elevated costing. Additionally, the appropriate immobilization material must also be carefully selected for specific biotransformation system as it is crucial for ensuring efficient immobilization¹⁷. Crude enzyme catalysis also evidently exhibited a lower half-life of PDC enzyme when compared with freeze-thawed whole cell biocatalyst¹⁸. The freezing and thawing technique was the preferred approach to break or cause leakage to the microbial cells such as yeasts with the distinct advantages over the alternative strategies with relative simplicity, cost-effectiveness, and robust performance^{6,18}. This method effectively deactivates alcohol dehydrogenase enzymes without compromising the stability of PDC enzyme on PAC biotransformation, thereby mitigating the formation of unwanted by-products from benzaldehyde such as benzyl alcohol and PAC-diol which was generally observed in live whole cell cultivation with simultaneous benzaldehyde addition, live whole cell immobilization system, or crude enzyme that was extracted directly from

the system without passing through the freezing and thawing process^{14,19–21}. Evidently, most of the original existing PDC enzyme activity was also well preserved for freeze-thawed whole cell biocatalyst⁶.

In recent times, ultrasound has found diverse applications in food and bioprocessing, encompassing activities such as crystallization, extraction, modification, quality control, functionality separation, meat processing, cell disruption, and microbial deactivation¹⁹. Ultrasound, characterized as sound waves with frequencies exceeding 18–20 kHz, can be categorized into three types: low frequency (20–100 kHz), high frequency (100–1000 kHz), and diagnostic ultrasound (1–500 MHz)²⁰. Low-intensity (<1 W/cm²) and high-frequency (2–10 MHz) ultrasound finds applications in medicine, ultrasound range finders, and electronic surface acoustic waves. On the other hand, high-intensity (>5 W/cm²) and low-frequency (20–100 kHz) ultrasound, or power ultrasound, induces lasting changes in the physical, chemical, or biological properties of materials or systems to which it is applied^{21–23}. Processes within the frequency range of 20–60 kHz often involve the widespread use of high-power ultrasound²⁴.

Similarly, the choice of the organic phase in addition to biocatalyst selection holds immense importance in the PAC biotransformation process. The organic phases such as vegetable oils (Vg-Oils), solvents, and other non-aqueous media serve as crucial components in two-phase systems^{25–28}, influencing the solubility and diffusion of substrates, products, and enzymes, overall reaction kinetics, as well as enzyme stability and activity^{29–33}. Thus, the primary objectives of the current study were to assess and compare cell disruption strategies with ultrasonication or glass beads attrition. The effects of three organic phases in the two-phase emulsion system, namely, Vg-Oil, Vg-Oil + dipropylene glycol (DPG), and octanol on overall PAC concentration, residual PDC activities, specific PAC production in relation to the initial volumetric PDC activity, PAC productivity, PAC yields as well as substrates molar balances were also elucidated. *C. tropicalis* TISTR 5306 could utilize longan extract as a carbon source for superior production of PAC and ethanol in comparison with the other *Candida* strains¹³. The effective disruption of frozen-thawed yeast whole cells (FT-WHC) by ultrasonication and their subsequent use in a two-phase emulsion system for improvement of PAC biotransformation has not been reported previously. The overall PAC concentration could be improved while the activities of the PDC enzyme were partially preserved through PDC stabilization and refolding.

Materials and methods

Fresh longan juice and FT-WHC preparations

Fresh longan fruits of C grade (dia. <1.9 cm) were obtained from a longan sorting center which was located in Saraphi District, Chiang Mai Province, Thailand. The center used an automated longan sorter machine (Model Yingruay, Likitchewan, Thailand) with a maximum sorting capacity of 40 t/day. The clear fresh longan juice (FLJ-C) of the fruit was obtained using a juice extractor (Model JE1, Febix, Thailand). *C. tropicalis* TISTR 5306 was provided by the Thailand Institute of Scientific and Technological Research (TISTR). The yeast strain was maintained in 40% (v/v) glycerol stock at –20 °C until used. Prior to the experiment, yeast cell viability was assessed by culturing on Yeast extract-Peptone-Dextrose (YPD) agar (in g/L; yeast extract 10, peptone 10, agar 20, and glucose 20) and subsequently grown in YPD broth at 30 °C, 250 rpm for 24 h. Yeast cell enumeration was conducted using a hemocytometer (Model PM MFR 650,030, Count Chamber, India) following staining with 0.1% (w/v) methylene blue to differentiate between live and dead cells, as per the method outlined by Borzani and Vairo³⁴. The yeast strain exhibited a viable cell count exceeding 95% and was employed as the starter culture, with an inoculation volume of 10% (v/v). The preparation of FT-WHC was previously described by Nunta et al.⁵ starting from cultivation conditions, cell harvesting, cell washing, and cell suspension with the corresponding volumetric PDC and specific PDC activities of 0.121 ± 0.004 U/mL and 0.410 ± 0.063 U/mg protein, respectively.

Cell disruption strategies

FT-WHC (12.24 g/L) was suspended in a 200 mM citrate buffer (pH 6.0/4.5 M KOH) for cells re-washing prior to centrifugation (2,822 × g for 15 min)⁶ and subsequent preparation in specific aliquot volume for each disruption strategy in 1 M phosphate buffer (pH 6.5/10 M KOH)⁹, namely, ultrasonication (Ult) and glass beads attrition (GBA). After cell-attrition processes, samples were then collected for the analyses of total protein concentration as well as volumetric and specific PDC activities. The best cell disruption technique was then chosen based on the Score Ranking Strategy⁵.

Ult method

An ultrasonic processor (Model VCX 500 Series, Sonics & Materials, United States), capable of operating at a maximum power output of 500 W and a frequency of 20 kHz was utilized. The sonicator utilized a horn-type standard probe with a threaded end tip (Part no. 630–0219; dia. 13 mm × length 136 mm). The ultrasonic probe had a processing volume ranging from 50 to 250 mL and ultrasonic amplitude modulation of 114 µm with the amplitude control set at 100%. Ultrasonic amplitude modulation levels were varied at 0% (FT-WHC), 20% (Ult20), 40% (Ult40), 60% (Ult60), 80% (Ult80), and 100% (Ult100). The sonication process was conducted in 100 mL aliquots of FT-WHC in a 200 mL glass jar (dia. 650 mm and height 850 mm) placed in an ice bath to minimize enzyme activity losses due to temperature increase. The sonication was performed in quintuplicate using a horn sonicator in the intermittent mode of 3 s ON and 7 s OFF, with a fixed total ON time of 3 min.

GBA method

Glass beads (GB) (0.55 mm diameter—Bio Pointe Scientific, Biospec 11,079,105, United States) were added to the FT-WHC suspension at a 1:1 mass ratio (w/w; g GB / g FT-WHC in buffer). The mixture underwent vortexing at 3000 rpm using a vortex mixer (Model VTX-3000L, Uzusio, Japan) for 1 min, followed by a cooling period in an ice/water mixture for three cycles with quintuplicate.

PAC production in two-phase emulsion system using non-disrupted and disrupted FT-WHC

Non-disrupted (control) and disrupted FT-WHC which was selected from the Cell Disruption Strategies Section were suspended in 1 M phosphate buffer (pH 6.5/10 M KOH) and utilized as biocatalysts for PAC production in a two-phase (organic/aqueous) emulsion biotransformation system using 250 mL Erlenmeyer flasks with the phase volume ratio of 1:1 (v/v). In the aqueous phase, sodium pyruvate at 240 mM with associated cofactors as described previously^{1,8,25} was added in a powder form to 50 mL of 1 M phosphate buffer in absence of non-disrupted FT-WHC (control aqueous phase) or disrupted FT-WHC which was already suspended in 1 M phosphate buffer. The equivalent volume of organic phase was used with 200 mM benzaldehyde dissolved in Vg-Oil. PAC biotransformation experiment with a total volume of 100 mL was conducted at 10.0 ± 1.0 °C and repeated four times. The addition of non-disrupted FT-WHC was done separately to the prepared control aqueous phase. The total reaction time was 240 min under emulsion form with a magnetic stirrer^{8,25}. Samples were collected in quintuplicate at sampling times of 0, 30, 60, 90, 120, 150, 180, 210, and 240 min. The biotransformation reaction was stopped by the addition of 100% (v/v) trichloroacetic acid and stored at -20.0 ± 1.0 °C for analyses of substrates, PAC, and by-products concentration using HPLC. The substrate's molar balance profiles were also assessed.

PAC production in two-phase emulsion system by varying types of organic phase

Similar PAC production system and conditions as described in the previous section were employed using the best cell disruption strategy that could produce whole cells biocatalyst for PAC biotransformation in two-phase emulsion system. The individual total working volume was 300 mL scale in a 500 mL Erlenmeyer flask. Three different organic solvents, namely, (1) Vg-Oil, (2) Vg-Oil + DPG (2.5 M DPG) (adapted from Leksawasdi et al.²⁸) and (3) octanol^{28,35}, were investigated. The total reaction time was now 360 min^{8,13} with sampling times of 0, 5, 10, 15, 20, 25, 30, 60, 90, 120, 150, 180, 210, 240, 270, 300, 330, and 360 min. The biotransformation reaction in one set of samples was stopped by exposure to an ice/water mixture and stored at -20.0 ± 1.0 °C for analysis of total protein concentration as well as volumetric and specific PDC activities. The cessation of reaction and storage for subsequent analyses of substrates, PAC, and by-products concentration using HPLC was done in the same way as elucidated in the former section.

Analytical methods

The measurement of dried biomass concentration was determined by assessing the weight difference^{4,8}. The concentrations of substrate (benzaldehyde), PAC, and by-products (benzoic acid and benzyl alcohol), along with PDC activities based on the carboligation reaction, were determined using HPLC with an Altima™ C8 column (Agilent Technologies, USA). The initial pH level was all set at 6.50 ± 0.01 (Rosche et al.³⁶) as this was considered the optimum value for PAC biotransformation. The monitoring of pH was carried out using a pH meter (Model pH 700, Eutech Instruments, Singapore). The detailed procedures for these analyses have been previously described^{4,8,9,13}. Volumetric PDC activity based on carboligase assay was defined as one unit, representing the amount of enzyme required to convert one μ mole of pyruvate and benzaldehyde substrates into an equivalent μ mole of PAC per min at 25 °C and pH 6.4³⁷. The total protein concentration was assessed utilizing the Bradford assay, employing bovine serum albumin as the protein standard³⁸. The specific carboligase activity, referred to as specific PDC activity, was quantified as the unit of PDC per mg protein (U/mg)^{5,37}. Substrate (pyruvate) and by-products concentrations from pyruvate (acetaldehyde and acetoin) were determined by HPLC using Zorbax C18 column, diode array detector (DAD) at 270 nm. Mobile phase containing 0.1% (v/v) trifluoroacetic acid and 2.2% (v/v) methanol in HPLC water, flow rate of 0.9 mL/min, pressure drop of 106–115 bar, and 50 °C for 25 min were employed⁵. The pyruvate and benzaldehyde molar balances were computed based on the strategy previously described^{4,5}. All chemicals were either analytical or HPLC grades. The score ranking strategy for the selection of the best disruption technique among other methods was based on a well-established scheme published previously^{5,25}. Initial and final PAC productivity ($Q_{\text{PAC,ini}}$ and $Q_{\text{PAC,fin}}$) were determined at 5 and 360 min by dividing PAC molar concentration with respective times. $Q_{\text{PAC,fin}}$ implied the productivity during which PAC concentration occurred at maximum level.

Statistical analysis

The measurements were performed in quintuplicate, and the reported results represented the average value \pm standard error (SE). Statistical analyses were conducted using the Statistical Packages for the Social Sciences (SPSS, version 17.0)³⁹. One-way Analyses of variance (ANOVA) were utilized, and Duncan's new Multiple Range Test (DMRT) was applied to compare means and ascertain statistical significance at a confidence level of 95% ($p \leq 0.05$)^{8,40}.

Results and discussion

Selection of biocatalyst with suitable cell disruption technique for higher PDC release

FT-WHC harvested after 48 h of batch cultivation in FLJ-C were utilized to compare cell disruption techniques, specifically high-power ultrasonication and GBA, for the release of intracellular PDC enzyme. High-power ultrasonication was employed for the whole cell disruption, using an ultrasonic processor capable of reaching a maximum power output of 500 W and an operating frequency of 20 kHz. The levels of ultrasonic amplitude modulation were adjusted to 0, 20, 40, 60, 80, and 100% (referred to as FT-WHC, and ultrasonically disrupted cells at Ult20, Ult40, Ult60, Ult80, and Ult100, respectively). The findings revealed that whole cells disrupted using the ultrasonication method had different impacts on protein concentrations and PDC activities compared to the FT-WHC. Notably, the protein concentrations increased with higher percentages of ultrasonic amplitude while the decreases in both volumetric and specific PDC activities were observed as illustrated in Fig. 1. This outcome aligned with a study by Lida et al.⁴¹, who investigated the release of intracellular protein from Baker's

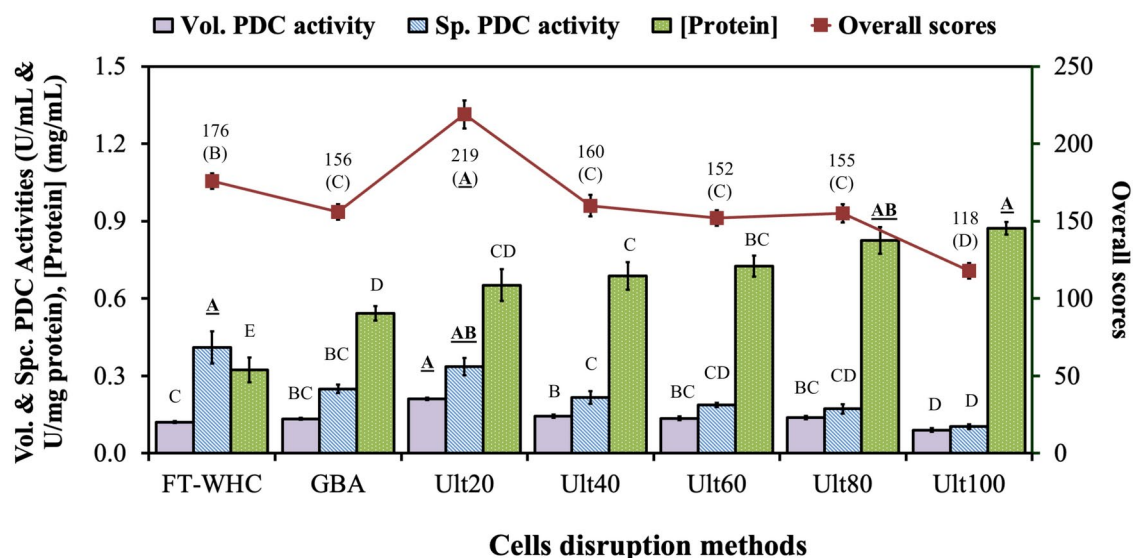


Fig. 1. Volumetric and specific PDC activities as well as overall scores of FT-WHC and disrupted FT-WHC obtained from various disruption methods. The numbers with the same capital alphabets indicated no significant ($p > 0.05$) difference across the specific group of pattern comparison.

yeast (*S. cerevisiae*) through ultrasonication. It was observed that the amount of released protein was directly linked to the increased sonication power within the lower power range (10 to 60 W), reaching a saturation point at higher power levels (> 80 W). The study identified an optimal point for Ult20 that resulted in the highest statistically significant ($p \leq 0.05$) volumetric PDC activity (0.210 ± 0.004 U/mL). The specific PDC activity was also highest (0.335 ± 0.033 U/mg protein) at this point, indicating that the released PDC enzyme remained active and retained its catalytic efficiency. This finding is crucial for biotransformation studies where the activity of the released enzymes is a critical factor. This could be explained by the cavitation phenomena which was a propagation of ultrasound in a medium resulting in the formation of cavitation bubbles⁴². Collapsing of these bubbles produced extreme temperature and pressure gradients, strong shear force, shock wave, as well as free radicals (OH , $\text{H}_2\text{O}^\bullet$ and O^\bullet)⁴³. Suslick and Crum⁴⁴ applied ultrasound in aqueous systems which generated acoustic cavitation with intense local heating (4000 – 5000 K), high pressures (1000 atm), enormous heating and cooling rates (> 109 K/s), and formation of liquid jet stream (400 km/h). Therefore, ultrasonication at the high percentage of amplitude or high ultrasonic intensity might have generated high temperature causing decreases in both volumetric and specific PDC activities while total protein concentration was unaffected.

The results of ultrasonication were compared with that of the GBA method which was considered as one of the successful means for cell disruption⁴⁵. The diameter of beads and loading concentration were important parameters in describing the degree of cell disruption. GB with 0.10 – 0.15 mm dia. were considered optimal sizes for disruption of bacteria while GB with 0.25 – 0.75 mm in diameter were used for the disruption of yeast cells^{46,47}. In the present study, GB with the size of 0.55 mm was used and the disrupted FT-WHC obtained from GBA had a total protein concentration of 0.542 ± 0.028 g/L which was relatively higher than FT-WHC but was lesser than ultrasonicated cells. While the volumetric PDC activity from GB (0.134 ± 0.004 U/mL) was statistically significant ($p \leq 0.05$) lower than the volumetric PDC activity of Ult20, it was not statistically significant different when compared with FT-WHC (0.121 ± 0.004 U/mL) and any other ultrasonicated cells from 40 – 100% amplitude. In contrast, the disrupted FT-WHC by GBA had specific PDC activity of 0.249 ± 0.017 U/mg protein which was statistically significant ($p \leq 0.05$) lower than that of FT-WHC (0.410 ± 0.063 U/mg protein) but was not statistically significant ($p > 0.05$) different from Ult20. The observed increase in volumetric PDC activity in the current study suggested a potential correlation with an enhancement in membrane permeability following ultrasonication treatment⁴⁸. Thus, ultrasonication could positively impact microbial cells by enhancing released PDC with notably higher specific PDC activity as elucidated by Tangtua⁶ who examined various methods for disrupting cells to liberate PDC from *C. tropicalis* TISTR 5350. Although ultrasonication revealed the highest efficiency of releasing intracellular biochemical compounds in microalgae (*Coelastrella* sp.) compared to bead milling, high-speed homogenization, and microwave treatment, bead milling might be considered the most effective technique when considering the balance of energy consumption and extraction efficiency⁴⁹. Additionally, Patil et al.⁵⁰ recognized that the synergistic impact of GBA and ultrasound from a bath sonicator served as an effective cell disruption method, leading to the release of intracellular arginine deiminase from *Pseudomonas putida*.

The selection of a biocatalyst based on the scores obtained from volumetric and specific PDC activities, and protein concentration of FT-WHC and various disrupted FT-WHCs are shown in Supplementary Table S1 and Fig. 1. The disrupted yeast whole cells obtained from the ultrasonication method at Ult20 was the most appropriate biocatalyst for higher PDC release as evidenced by the highest statistically significant ($p \leq 0.05$) total score of 219 ± 9 . FT-WHC had the second highest statistically significant ($p \leq 0.05$) total score (176 ± 5) while

disrupted FT-WHC obtained from Ult40 – Ult80 had total scores within the range of $152 \pm 5 - 160 \pm 7$ which were not statistically significant ($p > 0.05$) different from one another. The results also suggested that the cell disruption with GBA had a total score of 156 ± 5 which was statistically significant lower than both FT-WHC and Ult20 disrupted cells. Thus, the disrupted yeast whole cells obtained from the ultrasonication method at Ult20 and FT-WHC (control) were subsequently compared to assess the ability to produce PAC in a two-phase emulsion biotransformation system.

Comparison of PAC production from FT-WHC and disrupted FT-WHC using Ult20 in emulsion biotransformation systems

FT-WHC and disrupted FT-WHC obtained from Ult20 in suspension forms with 1 M phosphate buffer were used for PAC biotransformation in a two-phase emulsion system with initial volumetric and specific PDC activities as described in the previous section. The biotransformation study using FT-WHC as the biocatalyst investigated the PAC concentration levels at different time intervals and the results are shown in Table 1 and Fig. 2a. The results showed that at time zero, no PAC concentrations were being detected in either the Vg-Oil phase or buffer phase. PAC concentration gradually increased over time, reaching the highest statistically significant ($p \leq 0.05$) of $26.4 \pm 1.5 - 27.3 \pm 0.9$ at 210 – 240 min with $32.8 \pm 1.8 - 34.1 \pm 0.2$ mM presented in the Vg-Oil phase and $14.2 \pm 1.0 - 21.8 \pm 0.6$ mM in the buffer phase (Supplementary Table S2). The experiment also investigated the levels of residual substrates of pyruvate and benzaldehyde concentrations including benzoic acid concentration at different time intervals (Fig. 2a). The results showed that there was a decrease in the overall benzaldehyde concentration from 97.3 ± 1.2 mM initially to 70.9 ± 0.9 mM at 240 min. Pyruvate concentration decreased from 119 ± 3 mM to 91.9 ± 2.0 mM, while benzoic acid concentration increased to 2.69 ± 0.04 mM at 240 min. Benzaldehyde and pyruvate molar balances from emulsion biotransformation using FT-WHC of *C. tropicalis* were 77.6 ± 1.0 and $99.4 \pm 1.8\%$, respectively.

PAC concentration levels during biotransformation in a two-phase emulsion system using disrupted FT-WHC obtained from ultrasonication method at Ult20 as biocatalyst are shown in Table 1 and Fig. 2b. After 30 min, the overall PAC concentration level was observed to be 18.1 ± 0.5 mM. The results demonstrated that the overall PAC concentration levels increased over time, reaching to 25.5 ± 0.3 mM after 240 min, with 32.8 ± 0.4 mM resided in the Vg-Oil phase and 18.2 ± 0.6 mM in the buffer phase (Supplementary Table S3). Figure 2b presents the results investigating the concentration levels of residual benzaldehyde, pyruvate, and benzoic acid formation in the two-phase emulsion biotransformation system using Ult20 as a biocatalyst. The overall concentration levels of benzaldehyde decreased over time from 100 ± 1 mM initially to 70.8 ± 0.5 mM at 240 min. Similarly, the overall concentration levels of pyruvate also decreased over time, from 119 ± 0.4 mM at 0 min to 85.6 ± 0.3 mM at 240 min. However, the overall concentration levels of benzoic acid showed a slight fluctuation over time, ranging from 2.59 ± 0.03 mM to 3.27 ± 0.07 mM. The corresponding benzaldehyde and pyruvate molar balances were $96.3 \pm 0.4\%$ and $93.2 \pm 0.3\%$, respectively.

A comparison of PAC production using FT-WHC and disrupted FT-WHC at Ult20 as biocatalysts in emulsion biotransformation systems is shown in Table 2. The results indicated that the initial PAC production rate of biotransformation using Ult20 was statistically significant higher ($p \leq 0.05$) than using the FT-WHC as a biocatalyst. The Ult20 had initial PAC productivity of 3.26 ± 0.04 mM/min which was statistically significant higher ($p \leq 0.05$) than FT-WHC by twofold. This increased accessibility of PDC to its substrates, pyruvate, and benzaldehyde, facilitated a more efficient catalytic reaction, leading to higher initial PAC productivity. The disruption process likely exposed a larger surface area of PDC, making them readily available for catalysis, and enhanced mass transfer, allowing substrates to reach the active sites of the enzymes more effectively^{16,51,52}. Additionally, the improved permeability might contribute to a faster initiation of the biotransformation process, resulting in the higher initial PAC productivity.

Time (min)	Overall PAC (mM)		Q _{PAC} (mM/min)		Bz molar balance (%)		Pyr molar balance (%)	
	FT-WHC	Ult20	FT-WHC	Ult20	FT-WHC	Ult20	FT-WHC	Ult20
0	–	–	–	–	100 ^{Aa}	100 ^{Aa}	100 ^{Aa}	100 ^{Aa}
30	12.7 ^{Db}	18.1 ^{DEa}	0.424 ^{Ab}	0.602 ^{Aa}	71.8 ^{Db}	93.4 ^{BCa}	94.3 ^{Ca}	95.3 ^{CDEa}
60	13.8 ^{Db}	19.3 ^{CDa}	0.230 ^{Bb}	0.322 ^{Ba}	76.6 ^{BCb}	89.6 ^{Ca}	92.8 ^{Cb}	97.7 ^{Ba}
90	14.2 ^{Db}	17.3 ^{EFa}	0.158 ^{Cb}	0.198 ^{Ca}	78.8 ^{Bb}	99.2 ^{ABa}	87.9 ^{Eb}	96.1 ^{CDa}
120	19.0 ^{Ca}	18.7 ^{CDa}	0.159 ^{Ca}	0.156 ^{Da}	76.7 ^{BCb}	95.0 ^{ABCa}	88.8 ^{DEb}	95.4 ^{CDEa}
150	20.7 ^{BCa}	19.9 ^{Ca}	0.138 ^{Da}	0.132 ^{Eb}	77.8 ^{Bb}	95.3 ^{ABCa}	91.4 ^{CDb}	96.5 ^{BCa}
180	21.6 ^{Ba}	20.0 ^{Ca}	0.120 ^{EFa}	0.111 ^{Fb}	72.6 ^{CDb}	97.7 ^{ABa}	93.4 ^{Ca}	94.2 ^{EFa}
210	26.4 ^{Aa}	24.1 ^{Ba}	0.126 ^{Ea}	0.115 ^{Fb}	76.9 ^{BCb}	97.0 ^{ABa}	97.7 ^{Ba}	94.8 ^{DEa}
240	27.3 ^{Aa}	25.5 ^{Aa}	0.114 ^{Fa}	0.106 ^{Fb}	77.6 ^{BCb}	96.3 ^{ABa}	100 ^{Aa}	93.2 ^{Fb}

Table 1. Kinetic data of overall PAC produced, PAC productivity, as well as benzaldehyde and pyruvate molar balances in a two-phase emulsion (Vg-Oil/buffer) biotransformation system using FT-WHC and FT-WHC with Ult20 as biocatalyst. The numbers with the same capital alphabet indicate no significant ($p > 0.05$) difference for comparison of the same column. The numbers with the same small alphabet indicate no significant ($p > 0.05$) difference across the specific pair of pattern comparisons in the same row. All SE values were found to be less than 5% of average values are not shown in this table.

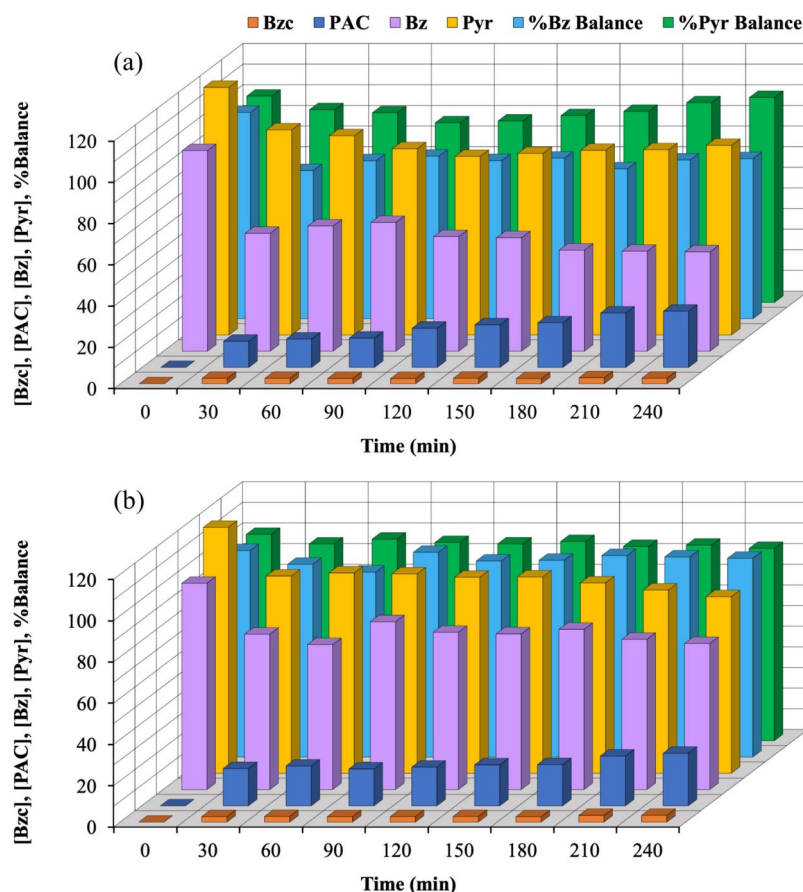


Fig. 2. Pyruvate (Pyr), benzaldehyde (Bz), PAC, and benzoic acid (Bzc) concentrations including Pyr and Bz molar balances in two-phase emulsion biotransformation system using (a) FT-WHC and (b) disrupted FT-WHC at Ult20 as biocatalyst. All SE values were found to be less than 5% of average values are not shown in this figure.

Cell disruption method	$Q_{PAC,ini}$ (mM/min)	$[PAC_{max}]$ (mM)	Bz molar balance (%)	Pyr molar balance (%)
FT-WHC	$1.54^B \pm 0.04$	$26.4 \pm 1.5^A - 27.3^A \pm 0.9$	$77.6^B \pm 1.0$	$99.4^A \pm 1.8$
Ult20	$3.26^A \pm 0.04$	$25.5^A \pm 0.3$	$96.3^A \pm 0.4$	$93.2^B \pm 0.3$

Table 2. Comparison of biocatalyst capability for initial PAC productivity, PAC concentration, benzaldehyde and pyruvate molar balances. The numbers with the same capital alphabet indicate no significant ($p > 0.05$) difference for comparison of the same column. Bold numbers indicated the highest statistically significant ($p \leq 0.05$) values in each row.

Further step for applying the current process on scale-up or industrial level would involve with sufficiency of evenly distributed sonication power on the suspension to be disseminated which is considered the principal limitation of an ultrasonication process⁵³. There are two other possible solutions that are currently available at a varying cost based on ultrasonication probe technology; (1) setting up the sonication probes in parallel or series for the pipe flow suspension which extend the residence time for dissemination with minimal effect on the process duration; (2) applying continuous flow ultrasonication with a circulating pump installed between a tank and a flow cell where ultrasonication process is applied to achieve acceptable energy and time efficiencies⁵⁴. Evidently, the relevant study of the ultrasonication process on the scale up level was done based on a continuous flow process on the pilot scale for chlorophylls and carotenoids extraction from plant with a slight drop in an extraction yield when compared to production on a smaller scale⁵⁵.

Comparison of different organic phases in PAC production with selected biocatalyst

The two-phase biotransformation method could effectively maintain a relatively low benzaldehyde concentration and toxicity in the aqueous phase where the PDC enzyme resided with gradual feeding of benzaldehyde from the organic phase based on partitioning equilibrium^{56,57}. PAC and by-products from benzaldehyde were also principally partitioned into the organic phase⁵⁸. This equilibrium partitioning helps prevent potential enzymatic

inactivation or inhibition from the toxicity of hydrophobic chemicals in the process, as demonstrated by Sandford et al.⁵⁹, Schmid et al.⁶⁰, and Leksawasdi et al.⁴, while elevating PAC production.

The pH profiles throughout the time course during PAC biotransformation in a two-phase emulsion system with different organic phases are shown in Fig. 3. The results indicated that pH levels of Vg-Oil/buffer and octanol/buffer were statistically significant ($p \leq 0.05$) decreased from 6.50 ± 0.01 to 6.34 ± 0.01 and 6.45 ± 0.01 , respectively when reaction time reached 360 min. In contrast, the pH of Vg-Oil + DPG/buffer system was even statistically significant ($p \leq 0.05$) higher reaching the value of 6.74 ± 0.01 at 360 min. The phenomenon observed in the latter system could be explained by the coupling proton consumption process that occurred simultaneously with PAC production hence resulting in the obvious pH rise when PAC concentration increased³⁶.

The total protein concentration was assessed to determine the effect of organic phase-type on the total protein concentration being released from the yeast cells throughout the biotransformation time course. It was observed that the initial protein concentration of all conditions was between 0.717 ± 0.034 and 0.728 ± 0.001 mg/mL as shown in Supplementary Figure S1. However, in due course of time, the octanol/buffer emulsion resulted in a statistically significant ($p \leq 0.05$) 85.6% decrease in total protein concentration leading to 0.105 ± 0.013 mg/mL which was statistically significant ($p \leq 0.05$) 56.4% and 51.8% lesser when compared with Vg-Oil/buffer and Vg-Oil + DPG/buffer respectively at the end of 360 min. The observed differences in total protein concentrations across different organic phases could be elucidated from enhanced release of total protein concentration from whole cells biocatalyst due to interaction with each organic phase causing variations in solubility and stability of PDC enzyme^{61,62}.

Volumetric and specific PDC activities of *C. tropicalis* during PAC biotransformation in a two-phase emulsion system of all conditions exhibited statistically significant ($p \leq 0.05$) decreases in relation to initial activities as shown in Fig. 4. The initial specific PDC activities were between 0.982 ± 0.038 and 1.08 ± 0.07 U/mg protein which were not statistically significant different ($p > 0.05$) from one another. However, at the end of the biotransformation process, the specific PDC activity was dropped by 67.8 and 66.8% from the initial counterpart in the Vg-Oil + DPG/buffer and octanol/buffer emulsions respectively. Similarly, mitigation of 83.3% in specific PDC activity for Vg-Oil/buffer emulsion was observed at the end of 360 min. The investigation of volumetric and specific PDC activities from disrupted *C. tropicalis* cells during PAC biotransformation in a two-phase emulsion system revealed that Vg-Oil + DPG and octanol emulsions had statistically significant ($p \leq 0.05$) improved stabilizing effects on PDC activity comparing with the Vg-Oil emulsion where DPG was absent. The inclusion of DPG could enhance enzyme stability by lessening water activity in the aqueous phase, similar to the effect achieved through glycerol addition used in many processes for enzyme stabilization⁶³. A previous study evaluated PDC deactivation kinetics in a biotransformation buffer with continuous exposure of various initial benzaldehyde concentrations in the range of 100 – 300 mM^{59,64}. A kinetic equation was proposed to describe this deactivation behavior whose deactivation rate constant was dependent on the benzaldehyde concentration while facilitating the selection of optimal benzaldehyde concentration level. Subsequently, Leksawasdi et al.⁶⁵ investigated the deactivation kinetics of partially purified PDC by benzaldehyde (0 – 200 mM) in 2.5 M 3-(N-Morpholino) propanesulfonic acid (MOPS) buffer. Experimental profiles showed that the enzyme activity decreased over time, with a lag period before deactivation occurred. A deactivation model was proposed, incorporating the effects of time, benzaldehyde concentration, and lag time. The study also compared PDC stability in different buffers and determined the half-life of PDC. Another study by Leksawasdi et al.²⁸ stressed that concentrated MOPS buffer (2.5 M) could maintain PDC stability but the relatively high cost of MOPS buffer resulted in cost inhibiting when applied to the industrial scale process. The improved enzymatic two-phase biotransformation for PAC production using 20 mM MOPS and 2.5 M DPG as an inexpensive replacement pair of high MOPS concentration. The inclusion of DPG as a solvent additive was effective in improvement of PAC

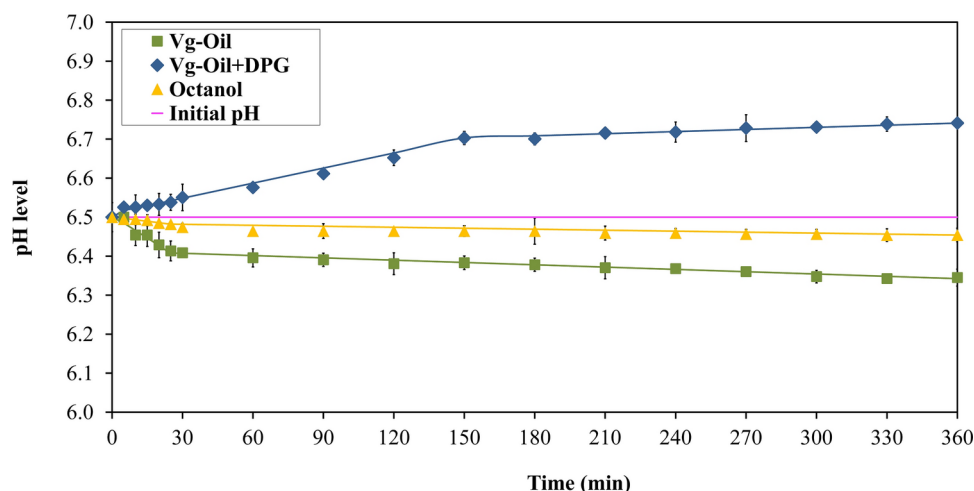


Fig. 3. pH profiles in multiple two-phase emulsion systems utilizing different organic phases for PAC biotransformation.

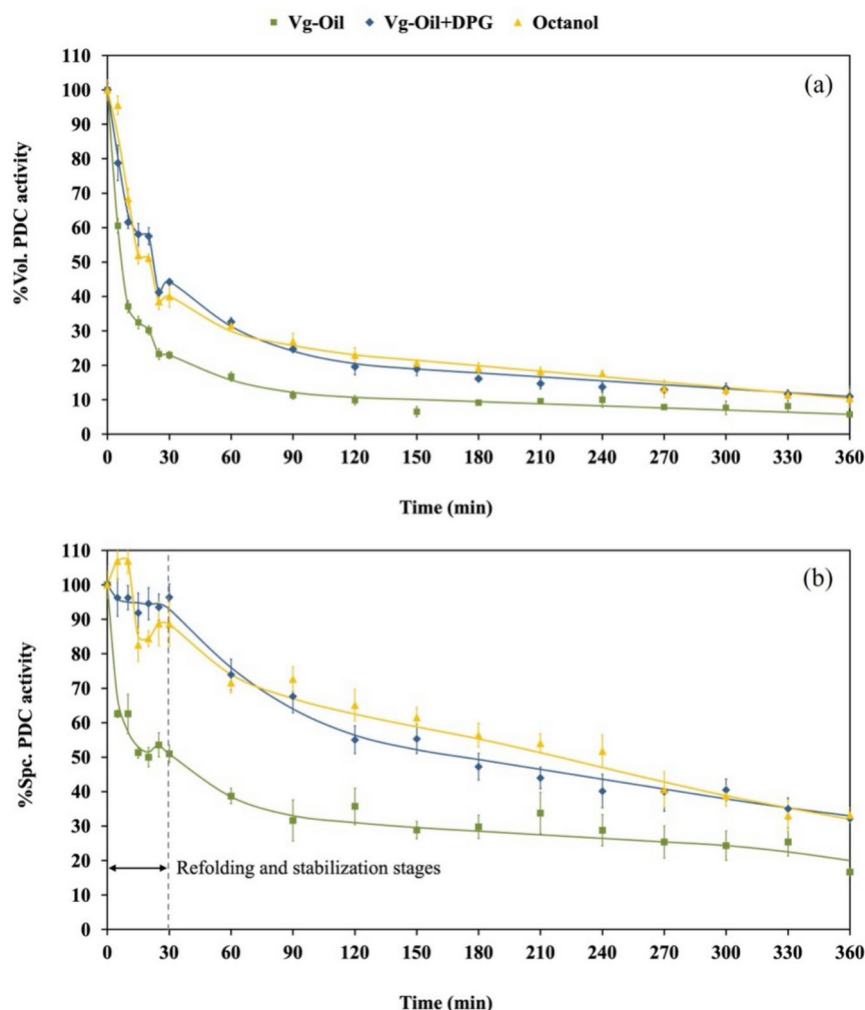


Fig. 4. Volumetric PDC activity (a) and specific PDC activity (b) of disrupted yeast whole cells (Ult20) during PAC biotransformation in a two-phase emulsion system with different organic phases.

formation rate through action of elevating PDC stability while favoring the benzaldehyde partitioning in the buffer phase²⁸.

The assessment of PAC production was conducted within the two-phase emulsion system, utilizing different organic phases as presented in Figs. 5, 6, 7. The kinetic profiles of PAC, benzaldehyde, pyruvate, and benzoic acid concentration were monitored throughout 360 min time course with the initial benzaldehyde (200 mM) and pyruvate (240 mM) concentrations residing in respective organic and aqueous phases of Figs. 5, 6, 7, respectively. The values at the initial time point represented the benzaldehyde or pyruvate concentration in each specific phase prior to mixing, thus its initial concentration in the counterpart phase was inevitably zero. The established equilibrium partitioning of benzaldehyde concentrations between organic and aqueous phases could be observed from 5 min thereafter. The corresponding equilibrium benzaldehyde concentrations in buffer phases of 16.3 ± 0.7 , 37.8 ± 0.5 , and 15.4 ± 0.5 mM were elucidated when Vg-Oil, Vg-Oil+DPG, and octanol were utilized as organic phases, respectively. These were contrary to pyruvate equilibria in respective organic phases where the relatively smaller average values of 0.75 ± 0.05 and 3.47 ± 0.30 mM were observed in Vg-Oil and octanol systems. Furthermore, the addition of DPG to the Vg-Oil+DPG system resulted in the gradual increase of pyruvate concentration in the organic phase due to the facilitating effect of DPG to dissolve polar compounds. The maximal value of up to 51.9 ± 1.4 mM pyruvate at 150 min was achieved before approaching the stable average value of 37.2 ± 1.4 mM. Figure 5 indicates the PAC production using Vg-Oil as the organic phase. The overall PAC concentration gradually increased over time in both Vg-Oil and buffer phases, reaching the highest statistically significant ($p \leq 0.05$) level of 22.9 ± 0.4 mM at 360 min. The PAC concentration levels found in Vg-Oil phase (34.2 ± 0.8 mM) were threefold higher when compared to that of the buffer phase (11.5 ± 0.1 mM). The corresponding residual benzaldehyde and pyruvate concentration levels at 360 min were 76.4 ± 4.4 and 83.4 ± 0.5 mM, respectively. The by-product, benzoic acid, formation was also detected during the PAC biotransformation process within the range of 0.036 ± 0.001 – 0.151 ± 0.002 mM. The computed benzaldehyde and pyruvate molar balances of 99.2 ± 4.4 and $88.5 \pm 0.5\%$ were determined, respectively.

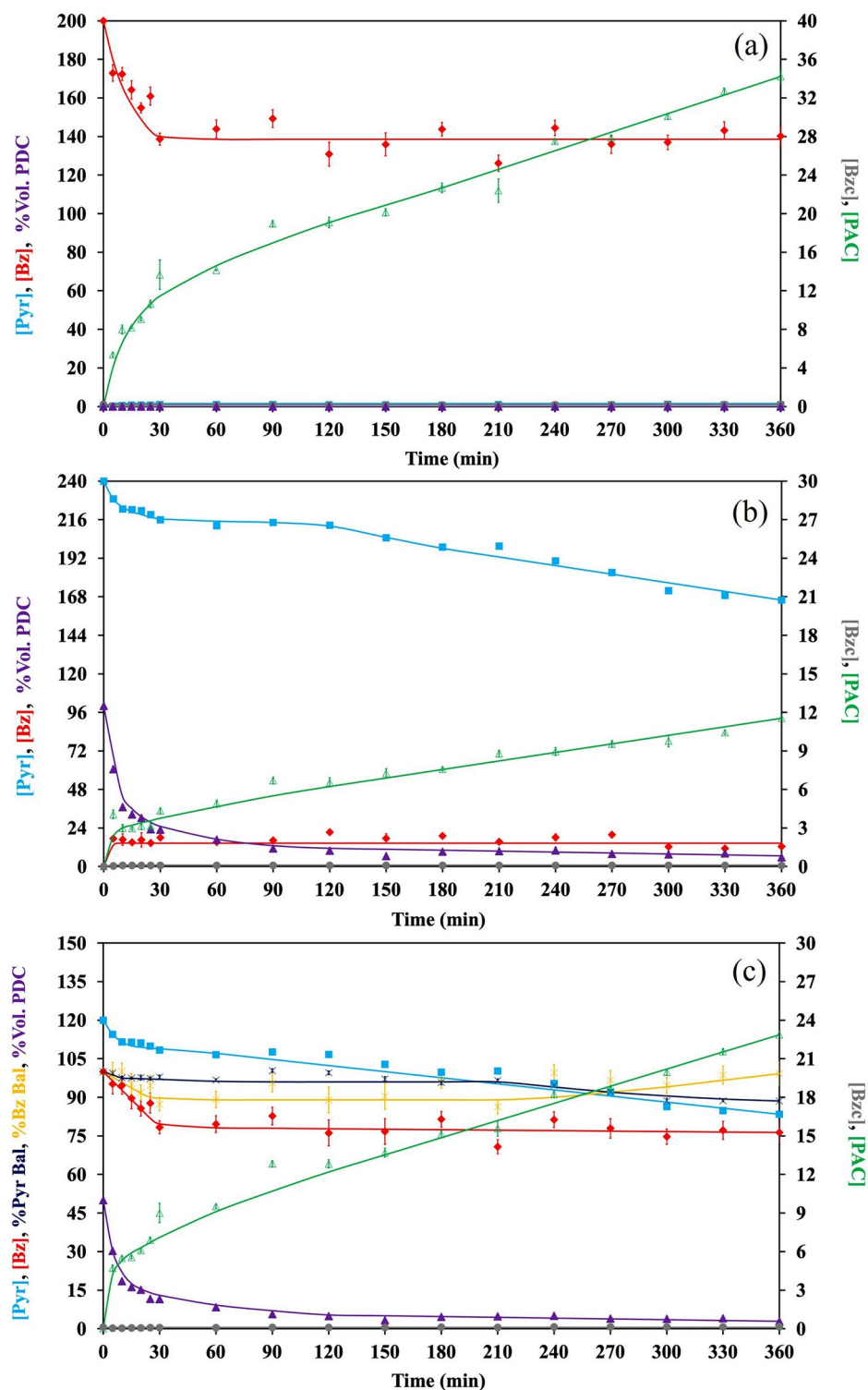


Fig. 5. Substrates (Pyr and Bz), product (PAC), and by-product (Bzc) concentrations including Pyr and Bz molar balances in (a) Vg-Oil phase, (b) buffer phase, and (c) overall phase from two-phase emulsion biotransformation system using disrupted FT-WHC with Ult20 as biocatalyst.

The present study also investigated the biotransformation of PAC in a two-phase emulsion system using Vg-Oil with DPG as the organic phase (Fig. 6). The results indicated that the PAC concentration levels gradually increased with each time increment in both phases reaching 32.1 ± 0.5 mM in the Vg-Oil + DPG phase and 25.8 ± 0.6 mM in the buffer phase at the end of 360 min. However, the PAC concentration level in Vg-Oil + DPG phase was statistically significant ($p \leq 0.05$) higher by 1.2-fold than that detected in the buffer phase. The corresponding overall PAC concentration of both phases reached 28.9 ± 0.1 mM while the corresponding

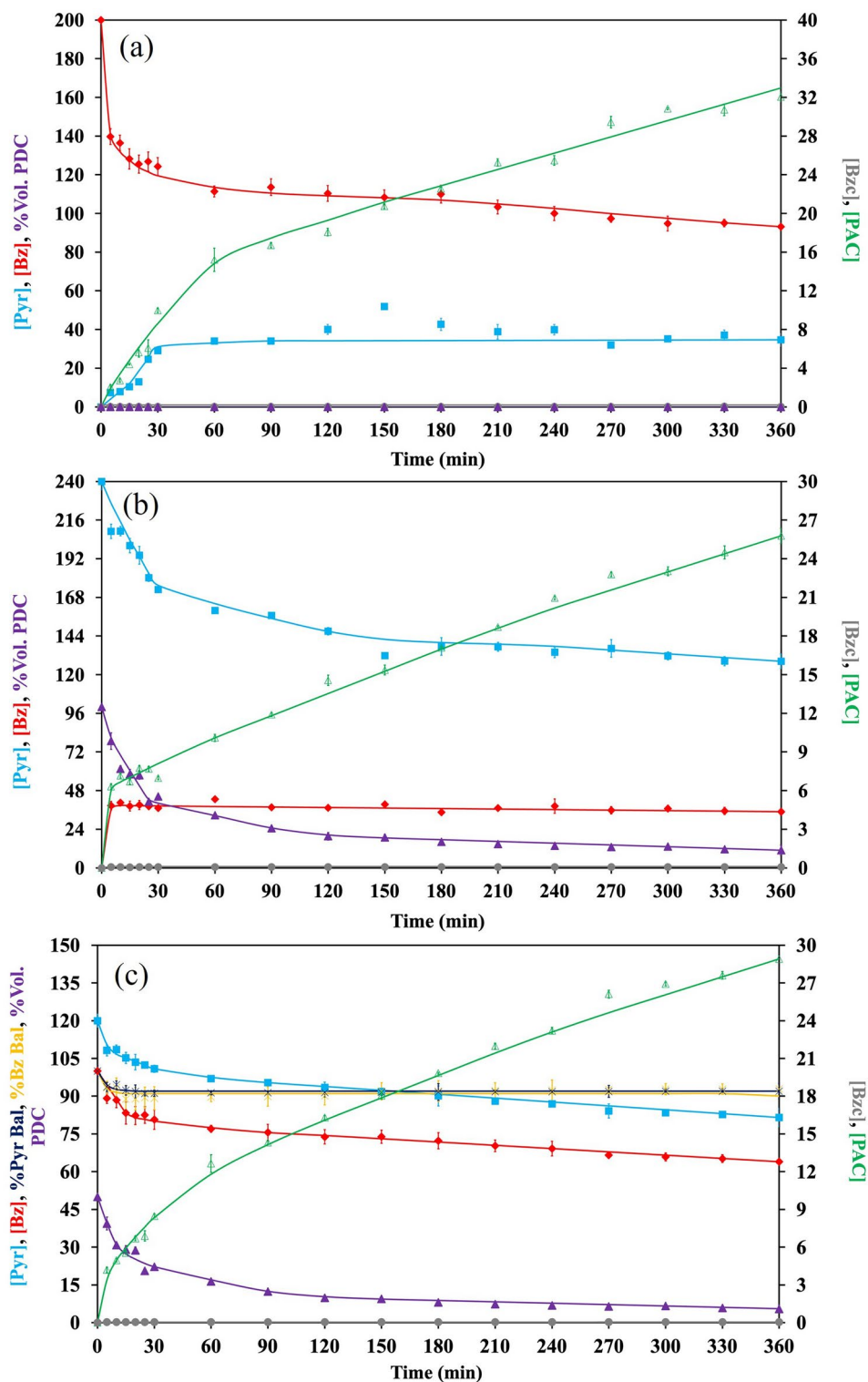


Fig. 6. Substrates (Pyr and Bz), product (PAC), and by-product (Bzc) concentrations including Pyr and Bz molar balances in (a) Vg-Oil + DPG phase, (b) buffer phase, and (c) overall phase from two-phase emulsion biotransformation system using disrupted FT-WHC with Ult20 as biocatalyst.

residual overall benzaldehyde and pyruvate concentrations were 64.0 ± 0.9 and 81.5 ± 3.6 mM, respectively. The benzoic acid formation was detected in the range of 0.033 ± 0.002 – 0.044 ± 0.001 mM which was relatively lower than that observed in Vg-Oil/buffer condition. The computed benzaldehyde and pyruvate molar balances of $92.9 \pm 1.2\%$ and $92.0 \pm 3.0\%$ were found, respectively.

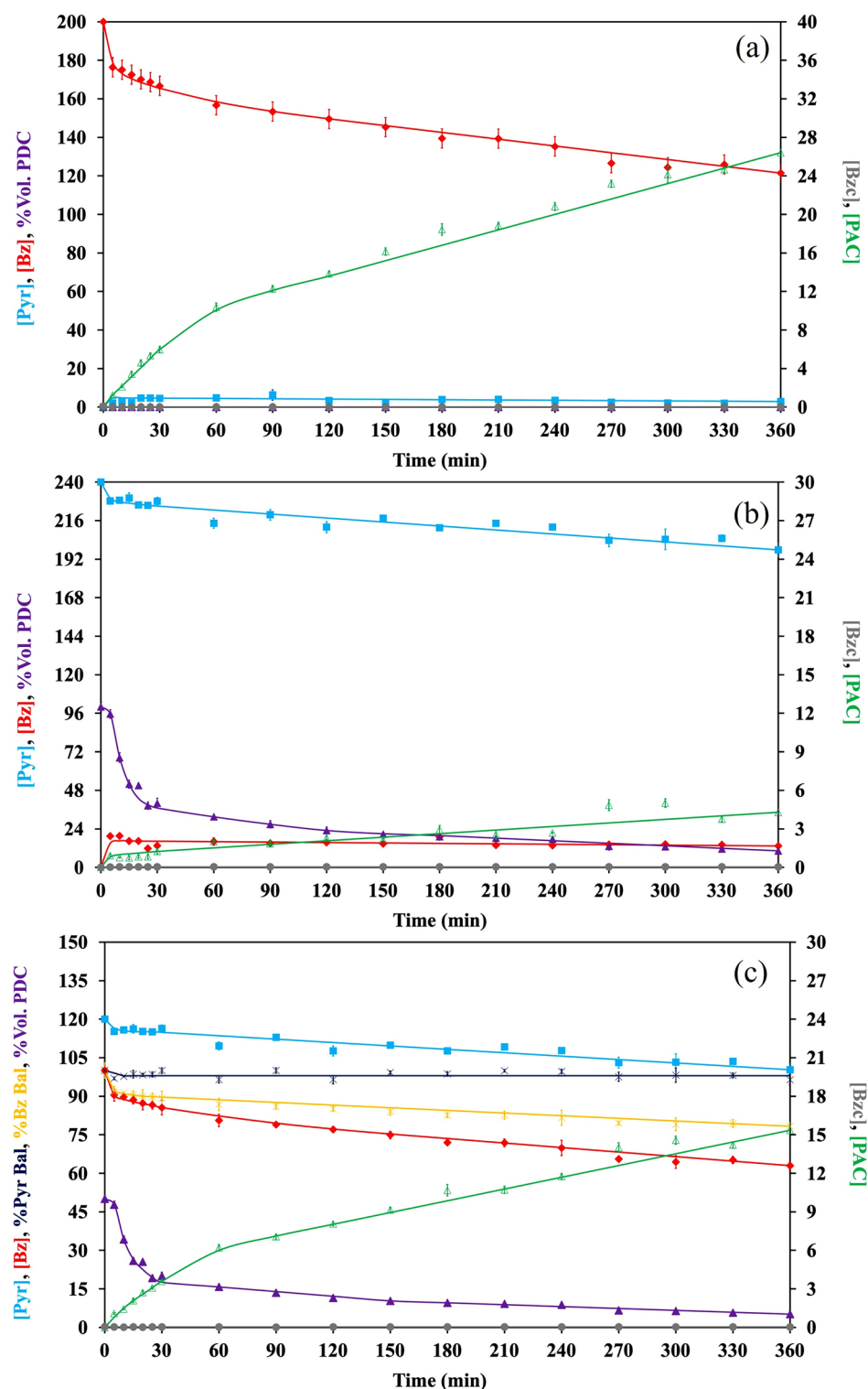


Fig. 7. Substrates (Pyr and Bz), product (PAC), and by-product (Bzc) concentrations including Pyr and Bz molar balances in (a) octanol phase, (b) buffer phase, and (c) overall phase from two-phase emulsion biotransformation system using disrupted FT-WHC with Ult20 as biocatalyst.

Octanol was also utilized as an organic phase to study the biotransformation process in the two-phase emulsion system (Fig. 7). The PAC concentration of 26.4 ± 0.4 mM was determined in the octanol phase while the buffer phase had a lower concentration of 4.30 ± 0.18 mM. PAC value in the octanol phase was thus statistically significant ($p \leq 0.05$) higher than that in the buffer phase by 6.1-fold with an overall PAC of 15.3 ± 0.2 mM. The corresponding residual overall benzaldehyde and pyruvate concentrations were 63.0 ± 1.4 and 100.3 ± 2 mM,

Variables	Two-phase emulsion systems of organic / aqueous phase			
	Vg-oil / Buffer *	Vg-oil / Buffer	Vg-Oil + DPG / buffer	Octanol / buffer
PAC _{org} (mM)	30.3 ^b ± 1.8	34.2^a ± 0.8	32.1 ^b ± 0.5	26.4 ^c ± 0.4
PAC _{aq} (mM)	24.1 ^b ± 1.0	11.5 ^c ± 0.1	25.8^a ± 0.6	4.30 ^d ± 0.18
PAC _{overall} (mM)	27.2 ^b ± 0.7	22.9 ^c ± 0.4	28.9^a ± 0.1	15.4 ^d ± 0.3
Residual Vol. PDC act. (%)	8.70^a ± 1.65	2.88 ^d ± 0.24	5.46 ^b ± 1.61	5.17 ^c ± 1.32
S _{p,PAC} (μmol/U _{ini})	97.1^a ± 2.5[†]	32.7 ^c ± 0.6	41.3 ^b ± 0.1	21.9 ^d ± 0.4
Q _{PAC,max} (mM/min)	0.076 ^d ± 0.002	0.944^a ± 0.050	0.838 ^b ± 0.042	0.216 ^c ± 0.014
Y _{PAC/Bz} (mol/mol)	0.667 ^c ± 0.019	0.967^a ± 0.020	0.803 ^b ± 0.001	0.414 ^d ± 0.008
Y _{PAC/Pyr} (mol/mol)	0.718 ^c ± 0.020	0.624 ^d ± 0.011	0.751 ^b ± 0.002	0.780^a ± 0.015
Pyr molar balance (%)	93.7^{ab} ± 1.2	88.5 ^c ± 0.5	92.0 ^{bc} ± 3.0	96.4^a ± 1.9
Bz molar balance (%)	83.1 ^c ± 1.5	99.2^a ± 4.4	92.9 ^b ± 1.2	78.3 ^d ± 1.4

Table 3. Comparison of PAC production in organic/aqueous two-phase emulsion systems. The numbers with the same alphabet indicate no significant ($p > 0.05$) difference for comparison of the same row. Bold numbers indicated the highest statistically significant ($p \leq 0.05$) values in each row. All variables were determined at 360 min except $Q_{PAC,max}$ whose values were determined at maxima. * The study from Nunta et al.⁵ that using *C. tropicalis* whole cells with specific PDC activity of 0.20–0.28 0.05 U/mg protein without ultrasonication treatment. † Calculation from reported overall PAC concentration and average value of initial specific PDC activity.

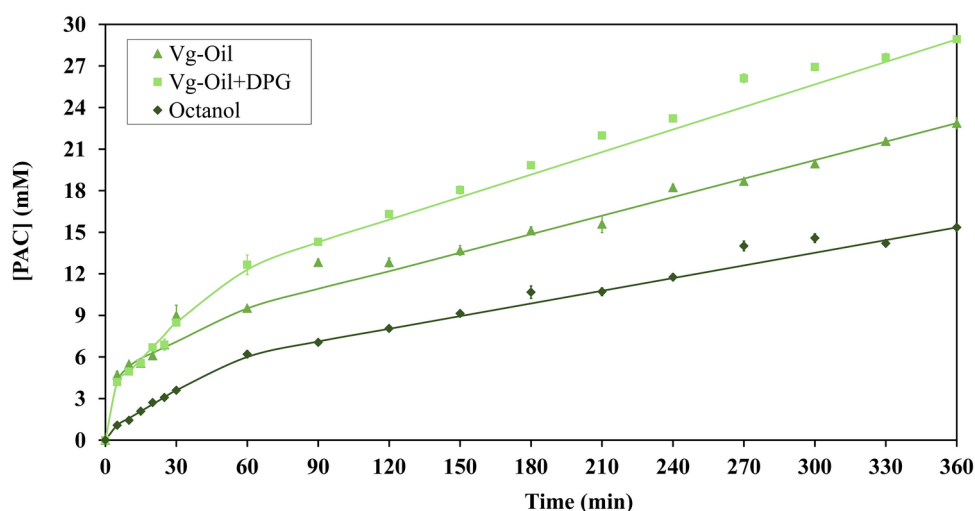


Fig. 8. Overall PAC concentration during biotransformation in the two-phase emulsion system with different organic phases.

respectively. The benzoic acid formation was detected in range of 0.016 ± 0.001 – 0.044 ± 0.031 mM. The benzaldehyde and pyruvate molar balances of $78.3 \pm 1.4\%$ and $96.4 \pm 1.9\%$ were determined, respectively.

Comparison of overall PAC concentrations obtained from biotransformation in two-phase emulsion system with different organic phases is shown in Table 3 and Fig. 8. The results indicated that the PAC concentrations were statistically significant ($p \leq 0.05$) different among the three both organic and aqueous phases. The Vg-Oil + DPG phase produced the highest statistically significant ($p \leq 0.05$) PAC concentration (28.9 ± 0.1 mM), followed by the Vg-Oil (22.9 ± 0.4 mM) and the octanol (15.4 ± 0.3 mM) phase. The residual volumetric activities of PDC in Vg-Oil + DPG and octanol ($5.17\% - 5.46\%$) were also statistically significant ($p \leq 0.05$) higher than that in Vg-Oil alone ($2.88 \pm 0.24\%$). Short terms PDC enzyme refolding effects as well as PDC stabilization effects due to the presence of octanol (1st stage: 0 – 10 min, 2nd stage: 15 – 30 min) or Vg-Oil + DPG (5 – 30 min) during the initial period of biotransformation were also evident during which specific PDC activities were maintained at constant levels or increased by certain extents before declining. The similar effect at the later stage of PAC biotransformation was observed for Vg-Oil system for a brief period (15 – 30 min) (Fig. 4). The results also supported that the two-phase emulsion system with Vg-Oil or Vg-Oil + DPG as the organic phases was a promising and eco-friendly method for PAC production. The relatively high partitioning of PAC into the aqueous phases was observed as shown in Table 3. PAC molar yield over benzaldehyde ($Y_{PAC/Bz}$) was highest statistically significant ($p \leq 0.05$) for Vg-Oil system while the PAC molar yield over pyruvate ($Y_{PAC/Pyr}$) appeared optimal in the octanol system. The maximum PAC molar productivity was highest statistically significant

($p \leq 0.05$) in the Vg-Oil system at 0.944 ± 0.050 mM/min. In earlier research, the introduction of glycerol in a two-phase emulsion biotransformation system could enhance PAC formation in the presence of benzaldehyde⁶⁶. Similarly, the addition of DPG also had the potential to improve the partitioning of benzaldehyde in a 20 mM MOPS system²⁸. The efficacy comparison of 2.5 M DPG + 20 mM MOPS to 2.5 M MOPS in octanol/aqueous two-phase biotransformation revealed the cost-effective substitute. This combination yielded comparable benzaldehyde concentration in the aqueous phase when compared to 2.5 M MOPS. PAC productivity and yield could be enhanced by utilizing 2.5 M MOPS or addition of DPG to low concentration MOPS system. The additional advantages of Vg-Oil + DPG system also included the statistically significant ($p \leq 0.05$) higher residual volumetric PDC activity ($5.46 \pm 1.61\%$) and specific PAC production per initial unit of PDC (41.3 ± 0.1 $\mu\text{mol}/\text{U}_{\text{int}}$). However, the maximum PAC productivity was observed for Vg-Oil only system.

The addition of DPG, polyol, is particularly advantageous as it can modify the dielectric constant of solvent systems, influencing micelle formation which creates a more compatible environment for enzyme–substrate interactions⁶⁷, contributing to the higher PAC concentration observed in the Vg-Oil + DPG system. Moreover, the stabilizing effect of DPG on enzyme structure helps to stabilize PDC enzymes during biotransformation, favoring higher PAC concentrations⁶⁸. Its stabilizing effect is attributed to the suppression of enzyme aggregation, driven by stronger polyol–protein interactions. Moreover, it can stabilize the secondary structure of enzymes at specific concentrations and elevated temperatures⁶⁸. By forming hydrogen bonds with the enzyme's surface, polyol preferentially excludes water from the protein's hydration shell, leading to a more compact enzyme structure while also preventing aggregation and degradation⁶⁹. For the biotransformation of PAC, stabilizing the enzyme PDC plays a key role in achieving high PAC concentration. The stabilizing effect of DPG enhances PDC stability, thereby facilitating higher PAC production.

This study reveals an advanced solvent system composed of Vg-Oil + DPG that increases the concentration of PAC compared to traditional systems using Vg-Oil and octanol alone. This innovative Vg-Oil + DPG mixture not only elevates PAC concentration but also significantly enhances enzyme stability. In addition, the utilization of Ult20-treated yeast cells accelerates the initial reaction rate, enabling a faster conversion process. The incorporation of DPG, a polyol, highlights its dual role as an effective extraction medium and a phase-modulating component in biphasic systems, further improving separation efficiency and biotransformation performance⁷⁰. This research offers insights into the synergistic effects of Vg-Oil + DPG, as well as the powerful application of ultrasonication to optimize enzyme-catalyzed biotransformation. Although the cost of ultrasonication at a large scale might be a consideration, it can be optimized by adjusting parameters or using more energy-efficient equipment, making it a viable approach for enhancing PAC production in industrial processes. Vg-Oil, widely recognized as an effective extraction medium for pharmaceutical compounds due to its extraction properties, further supports its role as a suitable biotransformation medium for large-scale experiments⁷¹.

From an environmental perspective, DPG exhibits favorable characteristics. It is non-volatile and readily dissolves in water, with a biodegradability of over 70% within 28 days. Also known as non-toxic and non-corrosive solvent⁷². Moreover, toxicological assessments have shown that DPG has low toxicity levels, making it suitable for use in biological systems. Studies on acute toxicity and developmental effects revealed no significant adverse effects at common exposure levels, with no evidence of genotoxic or carcinogenic effects in toxicity testing conducted on mice⁷³. While ionic liquids are recognized as green solvents, their high cost, recyclability challenges, and potential toxicity limit their industrial application⁷⁴. Similarly, deep eutectic solvents, though promising, face some limitations, including high viscosity, which can hinder mass transfer, as well as concerns regarding scalability and regulatory approval for industrial biotransformation⁷⁵ due to their recent development and much more research for the use of those solvents is needed.

The estimated chemical cost for PAC production was USD 255/kg PAC produced, as suggested by the estimation approach from Leksawasdi et al.⁷⁶. Such process did not include the biocatalyst costing as whole cells was considered as available by-product from the ethanol production step to be utilized in the zero-waste system. The implementation cost of ultrasonic step in this study has a beneficial effect of increasing the whole cells PDC activity from the original process by 1.74-fold after adopting FT-WHC thus mitigating the overall cost. Moreover, by applying the recycling procedure as suggested by Leksawasdi et al.⁷⁶, the overall costing could be mitigated to USD 66.4/kg PAC produced if the organic phase was recycled 4 times to accumulate PAC concentration. The overall PAC would then be improved from 28.9 mM to 116 mM after the fourth round. This could be compared to the PAC market value of USD 120/kg¹ hence signaling the economically viability and sustainability of such process. The added cost associated with the cell disruption process by implementing ultrasonication step could still be economical and effective on the scale-up production when compared to other disrupted processes^{6,49,54}. Even though the operational expenditure of ultrasonication system was 11% higher due to electricity consumption, capital expenditure could be 34% lower due to the compact design, with a 3% lower technical cost for each unit compared to the conventional design in the case of ultrasonic intensification for the CO₂ absorption process⁷⁷ that could be adapted to the current study.

Conclusions

This study highlighted that the disrupted whole cells obtained through ultrasonication at 20% amplitude combined with vegetable oil and dipropylene glycol as an organic solvent were the most suitable system for PAC biotransformation. Evidently, this novel system could maintain enzyme stability while improving PAC productivity as well as PAC partition. Further research into the underlying mechanisms linking ultrasound treatment, membrane permeability, and PDC activity could enhance understanding of industrial applications. It was evident that the inclusion of dipropylene glycol and vegetable oil, a non-toxic and competitive solvent, into organic phase contributed to the statistically significant ($p \leq 0.05$) enhanced PAC production, thus selection of suitable organic phase must be taken into consideration during the optimization of the PAC biotransformation process. Future works may include investigation relating to the effects of other green solvents such as deep

eutectic solvents and ionic liquids on PAC production and productivity on a large and industrial scales with augmentation of varied substrates feeding systems. The process techno-economic analysis or life cycle assessment can be evaluated and carried out using the parallel sonication probes in pipe flow system or continuous sonication system in order to extend the residence time in active dispersion zones and enhance production efficiency.

Data availability

The data sets generated during and/or analyzed during the current study are available from the corresponding authors on reasonable request.

Received: 19 September 2024; Accepted: 4 March 2025

Published online: 13 March 2025

References

- Porninta, K. et al. Pretreatment and enzymatic hydrolysis optimization of lignocellulosic biomass for ethanol, xylitol, and phenylacetylcarbinol co-production using *Candida magnoliae*. *Front. Bioeng. Biotechnol.* **11**, 2023 (2024).
- Parsaeimehr, A. & Sargsyan, E. *Natural Products* (Springer, 2013).
- Shin, H. S. & Rogers, P. L. Production of *L*-phenylacetylcarbinol (*L*-PAC) from benzaldehyde using partially purified pyruvate decarboxylase (PDC). *Biotechnol. Bioeng.* **49**, 52–62 (1996).
- Leksawasdi, N. et al. Kinetic analysis and modelling of enzymatic (*R*)-phenylacetylcarbinol batch biotransformation process. *J. Biotech.* **111**, 179–189 (2004).
- Nunta, R. et al. Ethanol and phenylacetylcarbinol production processes of *Candida tropicalis* TISTR 5306 and *Saccharomyces cerevisiae* TISTR 5606 in fresh juices from longan fruit of various sizes. *J. Food Process. Preserv.* **42**, e13815 (2018).
- Tangtua, J. Evaluation and comparison of microbial cells disruption methods for extraction of pyruvate decarboxylase. *Int. Food Res. J.* **21**, 1331–1336 (2014).
- Tangtua, J. et al. Evaluation of cell disruption for partial isolation of intracellular pyruvate decarboxylase enzyme by silver nanoparticles method. *Acta Aliment.* **44**, 436–442 (2015).
- Nunta, R. et al. Valorization of rice straw, sugarcane bagasse and sweet sorghum bagasse for the production of bioethanol and phenylacetylcarbinol. *Sci. Rep.* **13**, 727 (2023).
- Khemacheewakul, J. et al. Development of mathematical model for pyruvate decarboxylase deactivation kinetics by benzaldehyde with inorganic phosphate activation effect. *Chiang Mai J. Sci.* **45**, 1426–1438 (2018).
- Xu, Z. et al. Efficient bioreduction of ethyl 4-chloro-3-oxobutanoate to (*S*)-4-chloro-3-hydrobutanoate by whole cells of *Candida magnoliae* in water/*n*-butyl acetate two-phase system. *Biotechnol. Bioprocess Eng.* **11**, 48–53 (2006).
- Wachtmeister, J. & Rother, D. Recent advances in whole cell biocatalysis techniques bridging from investigative to industrial scale. *Curr. Opin. Biotechnol.* **42**, 169–177 (2016).
- Nagy-Győr, L. et al. Conservation of the biocatalytic activity of whole yeast cells by supported sol-gel entrapment for efficient acyloin condensation. *Period. Polytech. Chem. Eng.* **64**, 153–161 (2020).
- Tangtua, J. et al. Screening of 50 microbial strains for production of ethanol and (*R*)-phenylacetylcarbinol. *Chiang Mai J. Sci.* **40**, 299–304 (2013).
- Htike, S. L. et al. Production of xylitol and ethanol from agricultural wastes and biotransformation of phenylacetylcarbinol in deep eutectic solvent. *Agriculture* **14**, 2043 (2024).
- Saravana, P. S., Ummat, V., Bourke, P. & Tiwari, B. K. Emerging green cell disruption techniques to obtain valuable compounds from macro and microalgae: a review. *Crit. Rev. Biotechnol.* **43**, 904–919 (2023).
- Gautério, G. V. et al. Cell disruption and permeabilization methods for obtaining yeast bioproducts. *Clean. Chem. Eng.* **6**, 100112 (2023).
- Žur, J., Wojcieszynska, D. & Guzik, U. Metabolic responses of bacterial cells to immobilization. *Molecules* **21**, 958 (2016).
- Sharma, S. et al. A Simple and Cost-Effective Freeze-Thaw Based Method for *Plasmodium* DNA Extraction from Dried Blood Spot. *Iran J Parasitol.* **14**, 29–40 (2019).
- Ashokkumar, M. Applications of ultrasound in food and bioprocessing. *Ultrason. Sonochem.* **25**, 17–23 (2015).
- Zhang, B., Zhou, H., Cheng, Q., Lei, L. & Hu, B. Overexpression of HSP27 in cultured human aortic smooth muscular cells reduces apoptosis induced by low-frequency and low-energy ultrasound by inhibition of an intrinsic pathway. *Genet. Mol. Res.* **12**, 6588–6601 (2013).
- Paniwnyk, L. *Emerging Technologies for Food Processing* (Elsevier, 2014).
- Rokhina, E. V., Lens, P. & Virkutyte, J. Low-frequency ultrasound in biotechnology: state of the art. *Trends Biotechnol.* **27**, 298–306 (2009).
- Gallego-Juárez, J. *Ultrasound in Food Processing Recent Advances* (Wiley, 2017).
- O'Daly, B. J., Morris, E., Gavin, G. P., O'Byrne, J. M. & McGuinness, G. B. High-power low-frequency ultrasound: A review of tissue dissection and ablation in medicine and surgery. *J. Mater. Process. Technol.* **200**, 38–58 (2008).
- Kumar, A. et al. Production of phenylacetylcarbinol via biotransformation using the co-culture of *Candida tropicalis* TISTR 5306 and *Saccharomyces cerevisiae* TISTR 5606 as the biocatalyst. *J. Fungi* **9**, 928 (2023).
- Oliver, A. L., Anderson, B. N. & Roddick, F. A. Factors affecting the production of *L*-phenylacetylcarbinol by yeast: a case study. *Adv. Microb. Physiol.* **41**, 1–45 (1999).
- Feng, J. et al. Utilization of agricultural wastes for co-production of xylitol, ethanol, and phenylacetylcarbinol: A review. *Bioresour. Technol.* **392**, 129926 (2023).
- Leksawasdi, N., Rogers, P. L. & Rosche, B. Improved enzymatic two-phase biotransformation for (*R*)-phenylacetylcarbinol: Effect of dipropylene glycol and modes of pH control. *Biocatal. Biotransform.* **23**, 445–451 (2005).
- Fernandes, P. & Cabral, J. M. Biocatalysis in biphasic systems: general. *Org. Synth. Enzymes Non Aqueous Media* <https://doi.org/10.1002/9783527621729.ch8> (2008).
- Leon, R., Fernandes, P., Pinheiro, H. & Cabral, J. Whole-cell biocatalysis in organic media. *Enzyme Microb. Technol.* **23**, 483–500 (1998).
- Wang, S. et al. Enzyme stability and activity in non-aqueous reaction systems: a mini review. *Catalysts* **6**, 32 (2016).
- Carrea, G. & Riva, S. Properties and synthetic applications of enzymes in organic solvents. *Angew. Chem. Int. Ed.* **39**, 2226–2254 (2000).
- Baldascini, H., Ganzeveld, K. J., Janssen, D. B. & Beenackers, A. A. Effect of mass transfer limitations on the enzymatic kinetic resolution of epoxides in a two-liquid-phase system. *Biotechnol. Bioeng.* **73**, 44–54 (2001).
- Borzani, W. & Vairo, M. L. Quantitative adsorption of methylene blue by dead yeast cells. *J. Bacteriol.* **76**, 251–255 (1958).
- Agustina, A. et al. Screening of ethanol producing yeasts and bacteria in dried longan extract for the synthesis of *R*-phenylacetylcarbinol. *Asian J. Food Agro Ind.* **2**, 505–520 (2009).
- Rosche, B., Sandford, V., Breuer, M., Hauer, B. & Rogers, P. L. Enhanced production of *R*-phenylacetylcarbinol (*R*-PAC) through enzymatic biotransformation. *J. Mol. Catal. B Enzym.* **19**, 109–115 (2002).

37. Rosche, B. et al. Enzymatic (*R*)-phenylacetylcarbinol production in benzaldehyde emulsions. *Appl. Microbiol. Biotechnol.* **60**, 94–100 (2002).
38. Bradford, M. M. A rapid and sensitive method for the quantitation of microgram quantities of protein utilizing the principle of protein-dye binding. *Anal. Biochem.* **72**, 248–254 (1976).
39. Boonchuay, P. et al. Bioethanol production from cellulose-rich corncob residue by the thermotolerant *Saccharomyces cerevisiae* TC-5. *J. Fungi* **7**, 547 (2021).
40. Mahakuntha, C., Reungsang, A., Nunta, R. & Leksawasdi, N. Kinetics of whole cells and ethanol production from *Candida tropicalis* TISTR 5306 cultivation in batch and fed-batch modes using assorted grade fresh longan juice. *Anais Acad. Brasil. Ci.* <https://doi.org/10.1590/0001-3765202120200220> (2021).
41. Lida, Y., Tuziuti, T., Yasui, K., Kozuka, T. & Towata, A. Protein release from yeast cells as an evaluation method of physical effects in ultrasonic field. *Ultrason. Sonochem.* **15**, 995–1000 (2008).
42. Liu, L., Yang, Y., Liu, P. & Tan, W. The influence of air content in water on ultrasonic cavitation field. *Ultrason. Sonochem.* **21**, 566–571 (2014).
43. Baysal, T. & Demirdoven, A. *Ultrasound in Food Technology* (Handbook on Applications of Ultrasound: Sonochemistry for Sustainability, 2012).
44. Suslick, K. S. & Crum, L. A. *Sonochemistry and Sonoluminescence* (Wiley-Interscience, 1998).
45. Chen, L., Wang, J.-L., Ni, H. & Zhu, M.-J. Disruption of *Phaffia rhodozyma* cells and preparation of microencapsulated astaxanthin with high water solubility. *Food Sci. Biotechnol.* **28**, 111–120 (2019).
46. Schütte, H. & Kula, M.-R. Analytical disruption of microorganisms in a mixer mill. *Enzyme Microb. Technol.* **10**, 552–558 (1988).
47. Geciova, J., Bury, D. & Jelen, P. Methods for disruption of microbial cells for potential use in the dairy industry—a review. *Int. Dairy J.* **12**, 541–553 (2002).
48. Dong, W. et al. Ultrasound-assisted D-tartaric acid whole-cell bioconversion by recombinant *Escherichia coli*. *Ultrason. Sonochem.* **42**, 11–17 (2018).
49. Zhao, F., Wang, Z. & Huang, H. Physical cell disruption technologies for intracellular compound extraction from microorganisms. *Processes* **12**, 2059 (2024).
50. Patil, M. D. et al. Combined effect of attrition and ultrasound on the disruption of *Pseudomonas putida* for the efficient release of arginine deiminase. *Biotechnol. Prog.* **34**, 1185–1194 (2018).
51. Liu, Y., Liu, X., Cui, Y. & Yuan, W. Ultrasound for microalgal cell disruption and product extraction: A review. *Ultrason. Sonochem.* **87**, 106054 (2022).
52. Gomes, T. A., Zanette, C. M. & Spier, M. R. An overview of cell disruption methods for intracellular biomolecules recovery. *Prep. Biochem. Biotechnol.* **50**, 635–654 (2020).
53. Al-Juboori, R. A., Bowtell, L. A., Yusaf, T. & Aravinthan, V. Insights into the scalability of magnetostriptive ultrasound technology for water treatment applications. *Ultrason. Sonochem.* **28**, 357–366 (2016).
54. Girard, M., Bertrand, F., Tavares, J. R. & Heuzey, M.-C. A technique for the ultrasonic dispersion of larger quantities of cellulose nanocrystals with in-line validation. *Chem. Eng. J.* **446**, 137434 (2022).
55. Tamminen, J., Holappa, J., Vladimirovich Gradov, D. & Koironen, T. Scaling up continuous ultrasound-assisted extractor for plant extracts by using spinach leaves as a test material. *Ultrason. Sonochem.* **90**, 106171 (2022).
56. Santhanam, H. K. & Shreve, G. S. Solvent selection and productivity in multiphase biotransformation systems. *Biotechnol. Prog.* **10**, 187–192 (1994).
57. Karande, R., Schmid, A. & Buehler, K. Applications of multiphasic microreactors for biocatalytic reactions. *Org. Process Res. Dev.* **20**, 361–370 (2016).
58. Grundtvig, I. P. R. et al. Screening of organic solvents for bioprocesses using aqueous-organic two-phase systems. *Biotechnol. Adv.* **36**, 1801–1814 (2018).
59. Sandford, V., Breuer, M., Hauer, B., Rogers, P. & Rosche, B. (*R*)-phenylacetylcarbinol production in aqueous/organic two-phase systems using partially purified pyruvate decarboxylase from *Candida utilis*. *Biotechnol. Bioeng.* **91**, 190–198 (2005).
60. Schmid, A. et al. Industrial biocatalysis today and tomorrow. *Nature* **409**, 258–268 (2001).
61. Green, A. A. & Hughes, W. L. Protein fractionation on the basis of solubility in aqueous solutions of salts and organic solvents. *Methods Enzymol.* **1**, 67–90 (1955).
62. Dreyer, S., Salim, P. & Kragl, U. Driving forces of protein partitioning in an ionic liquid-based aqueous two-phase system. *Biochem. Eng. J.* **46**, 176–185 (2009).
63. Scopes, R. K. *Protein Purification: Principles and Practice* (Springer Science & Business Media, 1993).
64. Chow, Y., Shin, H., Adesina, A. & Rogers, P. A kinetic model for the deactivation of pyruvate decarboxylase (PDC) by benzaldehyde. *Biotechnol. Lett.* **17**, 1201–1206 (1995).
65. Leksawasdi, N., Breuer, M., Hauer, B., Rosche, B. & L. Rogers, P. Kinetics of pyruvate decarboxylase deactivation by benzaldehyde. *Biocatal. Biotransform.* **21**, 315–320 (2003).
66. Rosche, B., Breuer, M., Hauer, B. & Rogers, P. L. Role of pyruvate in enhancing pyruvate decarboxylase stability towards benzaldehyde. *J. Biotech.* **115**, 91–99 (2005).
67. Jiang, H., Beaucage, G., Vogtt, K. & Weaver, M. The effect of solvent polarity on wormlike micelles using dipropylene glycol (DPG) as a cosolvent in an anionic/zwitterionic mixed surfactant system. *J. Coll. Interface Sci.* **509**, 25–31 (2018).
68. Wang, X. et al. Polyethylene glycol Crowder's effect on enzyme aggregation, thermal stability, and residual catalytic activity. *Langmuir* **37**, 8474–8485 (2021).
69. Singh, S. & Singh, J. Effect of polyols on the conformational stability and biological activity of a model protein lysozyme. *AAPS PharmSciTech* **4**, E42 (2003).
70. Chen, J. et al. Application of poly (ethylene glycol)-based aqueous biphasic systems as reaction and reactive extraction media. *Ind. Eng. Chem. Res.* **43**, 5358–5364 (2004).
71. Cheikhoussef, N. & Cheikhoussef, A. *Green Sustainable Process for Chemical and Environmental Engineering and Science* (Elsevier, 2021).
72. Hu, J. & Wang, Z. L. Inhibition of water vapor condensation by dipropylene glycol droplets on hydrophobic surfaces via vapor sink strategy. *arXiv* **2311**, 03930 (2024).
73. Hooth, M. J. et al. Toxicology and carcinogenesis studies of dipropylene glycol in rats and mice. *Toxicology* **204**, 123–140 (2004).
74. Joseph, K. Navigating the pros and cons: Advantages and disadvantages of ionic liquids. *Polym. Sci.* **8**, 19 (2023).
75. Prabhune, A. & Dey, R. Green and sustainable solvents of the future: Deep eutectic solvents. *J. Mol. Liq.* **379**, 121676 (2023).
76. Leksawasdi, N. et al. *Asian Berries: Health Benefits Functional Foods and Nutraceuticals Series 123–148* (CRC Press, 2021).
77. Mohd Tamidi, A. et al. Numerical modeling and economic analysis of ultrasonic-assisted CO₂ absorption process for offshore application. *Processes* **11**, 3089 (2023).

Acknowledgements

The authors would like to thank funding supports from National Research Council of Thailand (NRCT) (Grant Number: NRCT5-RSA63004-08), Center of Excellence in Agro-Bio-Circular-Green Industry (Agro-BCG) (Grant Number: CoE67-P001), Office of Research Administration (ORA), Bioprocess Research Cluster (BRC), Faculty of Agro-Industry—Chiang Mai University (CMU). The present study was partially supported by the

Thailand Research Fund (TRF) Research Team Promotion Grant, RTA, Senior Research Scholar (Grant Number: N42A671052). TISTR is also thanked for microbial strain support.

Author contributions

Conceptualization, R.N. and N.L.; methodology, R.N., K.P. and N.L.; validation, R.N., K.P., A.K. and N.L.; formal analysis, R.N., J.K., K.P. and S.S.; investigation, R.N., K.P., C.M., J.F., S.L.H., U.B. and N.L.; resources, S.S. and N.L.; data curation, R.N., S.S., K.P., A.K. and N.L.; writing—original draft preparation, R.N., K.P. and A.K.; writing—review and editing, R.N., K.P., A.K., N.L., J.F., S.L.H., J.K., C.T., S.S., C.M., U.B., Y.P., P.R. and K.J.; supervision, A.K. and N.L.; project administration, N.L.; funding acquisition, N.L., C.T., Y.P., K.J. and P.R. All authors have read and agreed to the published version of the manuscript.

Declarations

Competing interests

The authors declare no competing interests.

Additional information

Supplementary Information The online version contains supplementary material available at <https://doi.org/10.1038/s41598-025-92947-0>.

Correspondence and requests for materials should be addressed to A.K. or N.L.

Reprints and permissions information is available at www.nature.com/reprints.

Publisher's note Springer Nature remains neutral with regard to jurisdictional claims in published maps and institutional affiliations.

Open Access This article is licensed under a Creative Commons Attribution-NonCommercial-NoDerivatives 4.0 International License, which permits any non-commercial use, sharing, distribution and reproduction in any medium or format, as long as you give appropriate credit to the original author(s) and the source, provide a link to the Creative Commons licence, and indicate if you modified the licensed material. You do not have permission under this licence to share adapted material derived from this article or parts of it. The images or other third party material in this article are included in the article's Creative Commons licence, unless indicated otherwise in a credit line to the material. If material is not included in the article's Creative Commons licence and your intended use is not permitted by statutory regulation or exceeds the permitted use, you will need to obtain permission directly from the copyright holder. To view a copy of this licence, visit <http://creativecommons.org/licenses/by-nc-nd/4.0/>.

© The Author(s) 2025